Electrodeposition of indium from a deep eutectic solvent

M. F. RAHMAN*, R. BERNASCONI, L. MAGAGNIN
Dipartimento di Chimica, Materiali e Ingegneria Chimica Giulio Natta
Politecnico di Milano, Via Mancinelli, 7 - 20131, Milan, Italy

(Received June 26, 2014; accepted January 21, 2015)

1. Introduction

Over the last two decades, low-temperature ionic liquids have received great attention [1-3] due to their wide applications in different research fields and applications such as electrodeposition, organic synthesis and chemical separations [4,5]. These ionic liquids generally demonstrate wide electrochemical window, where metals with very negative standard potentials can be deposited [6-12]. In addition, they exhibit good chemical and thermal stability, along with a good electrical conductivity. These low melting temperature (<100°C) ionic liquids are easier to work with compared to molten salts. Moreover, ionic liquids are nonvolatile and ideal replacement for traditional organic solvents that are volatile and flammable. However, the majority of the ionic liquids exhibits high sensibility to water or degradation by oxygen and needs a complex synthesis.

It has recently been found that the principle of creating an ionic fluid by complexing a halide salt can be applied to mixtures of quaternary ammonium salts with an amide, carboxylic acid or alcohol moiety [13-18]. These mixtures are called Deep Eutectic Solvent (DES). Such eutectic systems are easy to manipulate, nontoxic and biodegradable compared to room temperature ionic liquids. Furthermore, they demonstrate chemical inertness towards water and the production involves low costs and environmental risks.

The present study reports the electrochemical behavior of indium in one of these DES mediums (1:2 choline chloride/urea). The interest on novel electrodeposition methods for indium has increased recently because of its strategic importance. Indium is used in many engineering applications such as metal alloys for special uses, semiconductors for solar cells and electronic components. Many articles are available regarding electrochemical production of indium [19-21], while few articles are available regarding electrodeposition of indium from ionic liquids [22]. The present work is therefore intended to investigate the advantage of DES over other ionic liquids. A complete characterization of the plating process is reported, supported by electrochemical tests and nucleation studies on different substrates.

2. Experimental

Choline chloride (ChCl) (Sigma-Aldrich) and Urea (U) (Sigma-Aldrich) were used as received. The Deep Eutectic Solvent (DES) was formed by stirring ChCl and U together in a 1:2 molar ratio at 80°C until a homogeneous, colourless liquid is formed. Indium sulfate (Sigma-Aldrich) was used for the deposition of indium. A three-electrode cell was used for electrochemical experiments. For the cyclic voltammetry, the working electrode was gold (Au) with scan rates 2, 5, 10 mV/s. For chronoamperometry gold (Au) and molybdenum foil (Mo) were used as working electrodes. Platinum (Pt) wire and Titanium mesh (Ti) were used as reference electrode and counter electrode respectively. Electrodeposition experiments were conducted on a standard single compartment, two-electrode system, using Mo foil as substrate. Au, Pt wire and Ti mesh were ultrasonically cleaned in acetone and then distilled water each for 10 minutes prior to use. Mo foil was first ultrasonically cleaned in acetone for 10 minutes, then pretreated for 20 minutes in 32% HCl and finally ultrasonically cleaned in water for 10 minutes. The deposits were washed with distilled water and dried under nitrogen. $In_2(SO_4)_3$ 50mM solution was employed for all the experiments. Work temperature was kept constant at 80°C to lower the viscosity and maintain high conductivity of the solvent. Cyclic voltammetry and chronoamperometry experiments were carried out using an EG&G Princeton Applied Research Corporation (PAR)

*Contact author: md.farabi@mail.polimi.it

model 273A potentiostat controlled by EG&G PAR model 270 software. The surface morphology of the deposits was examined by scanning electron microscopy (SEM, Zeiss EVO50), and the chemical composition was determined by energy dispersive spectroscopy (EDS). The crystallinity of the deposits was analysed by X-ray diffraction Philips PW 1830, in conventional Bragg–Brentano configuration with Cu Ka radiation of 1.5418 Å wavelength. UBM laser profilometer MICROFOCOUS was used to determine roughness of indium deposit on molybdenum.

3. Results and discussion

The initial electrochemical study was executed by carrying out cyclic voltammetric experiments. Fig. 1(a) shows cyclic voltammograms at different scan rates of the cathodic zone. At high scan rate (10 mV/s) two reduction peaks are evident near -1.1 V and -0.9 V. On the contrary, at lower scan rate (2 mV/s) one reduction peak is visible in the zone close to -0.7 V. The voltammograms exhibit weird behaviour for scan rate 5 mV/s. On the other hand, voltammograms show typical behaviour (negative shift in the cathodic peak potential with increasing scan rate) for scan rates 2 mV/s and 10 mV/s. The negative shift in the cathodic peak potential with increasing scan rate reveals that this may be a slow charge-transfer reaction and/or an overpotential required nucleation in a quasi-reversible reaction condition. This behaviour was also observed in previous research of indium in ionic liquids [22]. Voltammograms also exhibit the typical reduction/oxidation loop of electrodeposition processes requiring nucleation overpotential.

Fig. 1(b) shows cyclic voltammograms at different scan rates in larger potential range. For all cathodic limits used a single anodic peak is evident at different scan rates. Also the position of this anodic peak is variable and is comprised in the -0.6 V/-0.3 V regions. Chronoamperometry experiments were performed at Au and Mo electrodes in order to investigate the nucleation/growth process for the electrodeposition of indium. These experiments were executed by stepping the potential of the working electrode from values at which no reduction of In(III) would occur to potentials sufficiently negative to initiate reduction. Fig. 2 reports the current-time transients, characterized by the typical shape for nucleation process. Here I_m, represents maximum current density and the corresponding time is represented by t_m. After t_m, the current starts to decrease due to the increase of the diffusion layer thickness. These transients also suggest that after t_m the growth of indium nuclei is diffusion controlled.

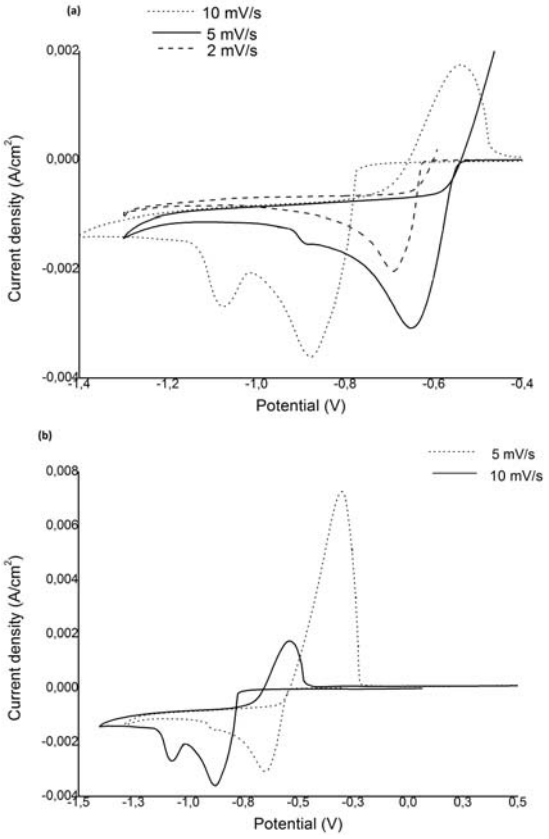

Fig. 1. Cyclic voltammograms in 50mM $In_2(SO_4)_3$ solution (a) at the cathodic zone, (b) at larger potential range on gold.

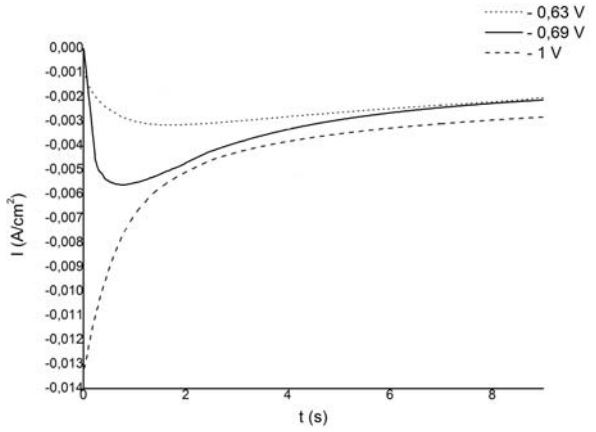

Fig. 2. Current - time transients resulting from chronoamperometry experiments recorded at Mo electrode in 50 mM $In_2(SO_4)_3$ solution at 80°C.

To determine the type of nucleation, the current-time transients were normalized and compared to the theoretical dimensionless current-time transients obtained from Scharifker-Hills model [23]. Fig. 3(a) shows the experimental and theoretical curves at -0.69V for Mo electrode. It is evident that the electrodeposition of indium on Mo substrates follows the three-dimensional instantaneous nucleation process. On the contrary, Fig. 3(b) exhibits that the electrodeposition of indium on the gold substrate at -0.69V follows the progressive nucleation mechanism. Although the latter demonstrates conformity to the model in the first instants of the nucleation, at higher values of t/t_m it shows a significant deviation from the predicted diffusion limited current.

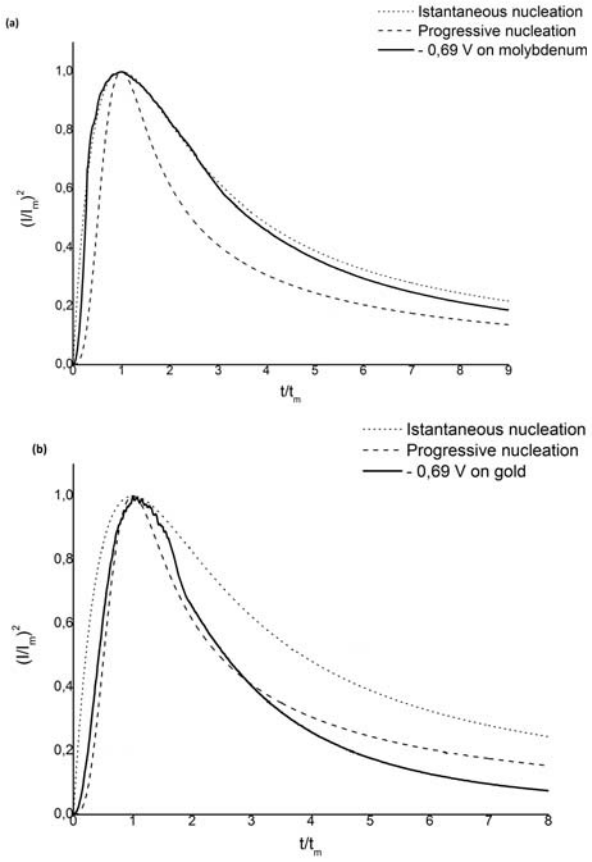

Fig. 3. Comparison of the dimensionless experimental current-time transients derived from the chronoamperometric experiments (a) at molybdenum electrode, (b) at gold electrode.

In order to understand the deviation from theoretical model on Au electrode, further investigation was done with SEM. Three samples were prepared with deposition time 1s, 2s and 3s respectively. Fig. 4 shows the micrographs of the three samples.

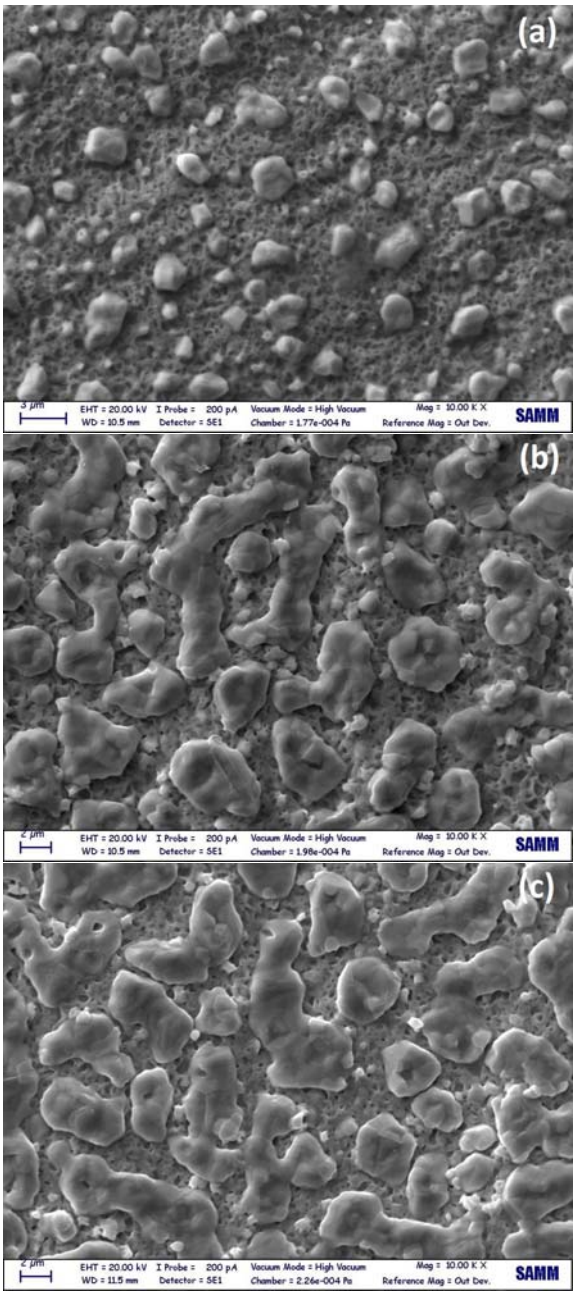

Fig. 4. SEM micrographs of the deposits prepared in 50 mM $In_2(SO_4)_3$ solution on gold with deposition time (a) 1s, (b) 2s and (c) 3s.

It is evident from the micrographs that the nucleation of indium at Au electrode proceeds progressively via formation of small nuclei that subsequently merge together to form In islands (Fig.4 (a), (b) and (c)). The observed mechanism presents key differences with respect to a standard progressive nucleation where coalescence of the nuclei occurs along with nucleation (Fig. 4(b) and (c)). The reason of the deviation from the predictions of the Scharifker-Hills model should take into account also the low melting point of indium compared to the temperature

of the electrolyte, probably favoring the coalescence of the nuclei.

Bulk electrodeposition of indium was carried out at 80°C on thin molybdenum (Mo) foil in 50 mM $In_2(SO_4)_3$ solution at different current densities. EDX analysis of the electrodeposits demonstrates that they are very pure deposits of In and there are no contaminants like Cl, O trapped in the deposits from deep eutectic solvent (Fig. 5(a)). XRD diffractograms of the deposit exhibit the presence of crystalline indium (Fig. 5(b)) with a preferential orientation along the (101) plane.

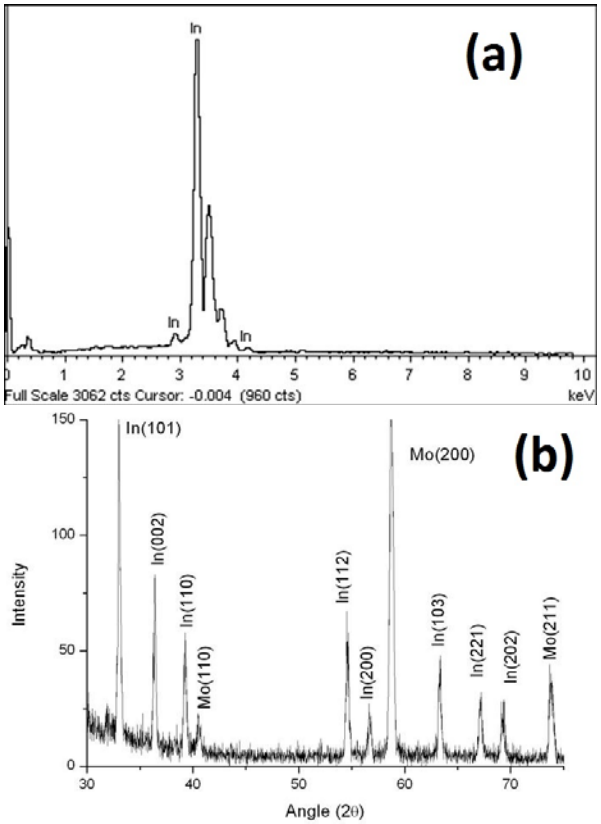

Fig.5. (a) EDX spectrum and (b) XRD pattern of In deposits in 50 mM $In_2(SO_4)_3$ solution at current density 10 mA/cm^2 after 60 minutes of deposition on molybdenum.

The morphology of the deposits on Mo was investigated with SEM. At lower current density (Fig. 6(a) and (b)), the micrograph shows polygonal shaped grains having an average grain size of 6 µm. At higher current density (Fig. 6(c)) the deposit exhibits nodular morphology with rounded grains. The average grain size is 2 µm with increasing coverage of the substrate. Grains become fine at higher current density which reflects an increase in the indium nuclei density with increasing deposition current density.

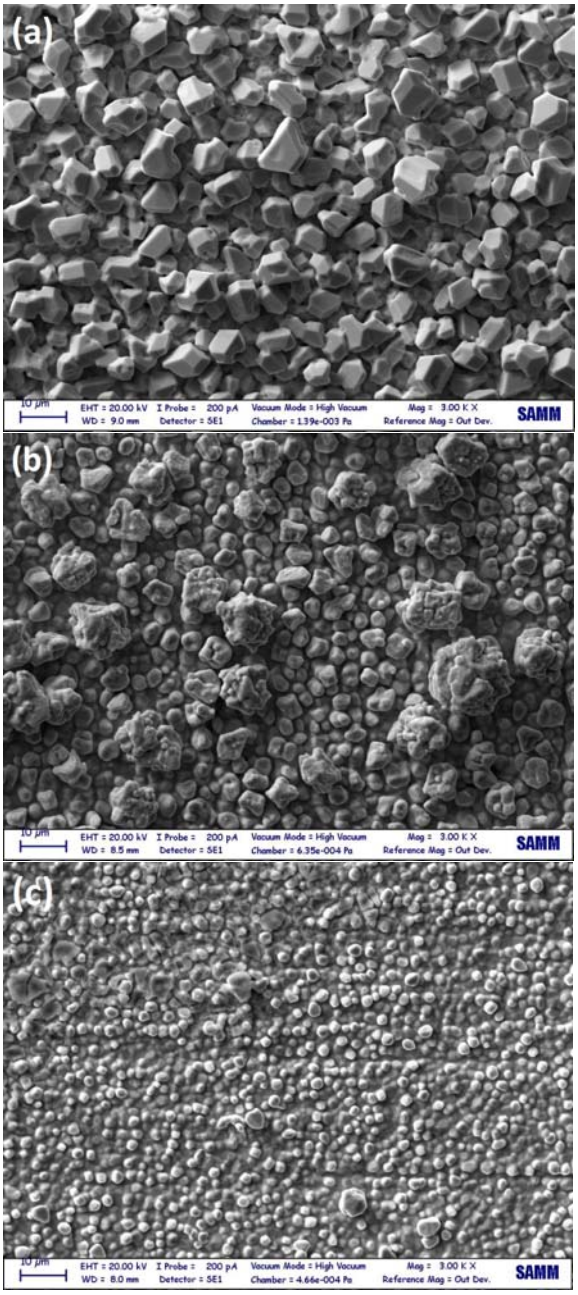

Fig. 6. SEM micrographs of the deposits in 50 mM $In_2(SO_4)_3$ solution on molybdenum at current density (a) 10 mA/cm^2, (b) 30 mA/cm^2, (c) 50 mA/cm^2.

The deposits show high roughness values at low current densities. Table1 shows the average roughness values of the three deposits, with a decrease as the current density increases.

Table 1 Average roughness of the indium deposits obtained at different current densities.

Current density (mA/cm^2)	Deposition time (minutes)	Average Roughness, R_a (μm)
10	40	0.41
30	40	0.39
50	40	0.31

4. Conclusions

In this paper the electrodeposition of indium was investigated in DES electrolyte, and the results show the possibility of electrodeposition of pure crystalline indium. Electrodeposition of indium at Mo electrode proceeds via instantaneous nucleation with diffusion-controlled growth whereas the deposition at Au electrode proceeds via progressive nucleation. The surface morphology of the deposits improves at higher current density, with a decrease of the surface roughness. Further investigation can be done in order to enhance surface morphology of the deposit considering several applications of indium.

References

[1] M.J. Earl, K.R. Seddon, Pure Appl. Chem., **72**, 1391 (2000).

[2] C.L. Hussey, G. Mamantov, In Chemistry of Nonaqueous Solutions Current Progress; Popov, AI, Eds, VCH; NewYork, 1994; p 227.

[3] J.S. Wilkes, J.A. Levisky, R.A. Wilson, C.L. Hussey, Inorg. Chem., **21**, 1263 (1982).

[4] (a) G.R. Stafford, C. Hussey, RC. Alkire, In Advances in Electrochemical Science and Engineering; Kolb, DM., Eds.; Wiley-VCH; **7**, 275 (2001) (b) Welton T. Chem. Rev. **99**, 2071 (1999).

[5] I.W. Sun, S.Y. Wu, C.H. Su, Y.L. Shu, P.L. Wu, J. Chin. Chem. Soc. 2003.

[6] A. Lisenkov, M.L. Zheludkevich, M.G.S. Ferreiro, Electrochem. Comm. **12**(6), 729 (2010).

[7] F. Xiao, F. Zhao, D. Mei, Z. Mo, B. Zeng, Biosens. Bioelectron. **24**, 3481 (2009).

[8] A.P. Abbott, K.J. McKenzie, Phys. Chem. Chem. Phys. **8**, 4265 (2006).

[9] S. Zein El Abedin, A.Y. Saad, H.K. Farag, N. Bousenko, Q.X. Liu, F. Endress, Electrochim. Acta **52**(8), 2746 (2007).

[10] F. Endres, D. MacFarlane, A.P. Abbott, Electrodeposition from Ionic Liquids, Wiley-VCH Verlag GmbH, Weinheim, Germany, 2008.

[11] J. Tang, K. Azumi, Electrochim. Acta **56**(3), 1130 (2011).

[12] E. Gómez, P. Cojocaru, L. Magagnin, E. Valles, J. Electroanal. Chem. **658**, 18 (2011).

[13] A.P. Abbott, G. Capper, D.L. Davies, R. Rasheed, V. Tambyrajah, Chem. Commun. 70 (2003).

[14] A.P. Abbott, G. Capper, B.G. Swain, D.A. Wheeler, Trans. Inst. Met. Finish. **83**, 51 (2005).

[15] A.P. Abbott, G. Capper, K.J. McKenzie, K.S. Ryder, J. Electroanal. Chem. **599**(2), 288 (2007).

[16] A. Florea, L. Anicai, S. Costonci, F. Golgovici, T. Visan, Surf. Interface Anal. **42**, 1271 (2010).

[17] M.S. Zebarjadi, Copper electrodeposition from deep eutectic solvents for TSV technology. MS. Thesis. (2013), Politecnico di Milano, Italy.

[18] S. Xing, C. Zanella, F. Deflorian, J. Solid State Electrochem. **18**(6) 1657 (2014).

[19] A. Brenner, Electrodeposition of Alloys, Principles and Practice; Academic: New York, 1963; p 547.

[20] N. Miani, Indium deposition for transparent and flexible devices. MS. Thesis. (2013), Politecnico di Milano, Italy.

[21] A.V. Oriani, Synthesis of indium phosphide for thin film solar cells. MS. Thesis. (2013), Politecnico di Milano, Italy.

[22] M.H. Yang, I.W. Sun, J. Chin. Chem. Soc. **51**, 253 (2004).

[23] B. Scharifker, G. Hills, Electrochim. Acta. **28**, 879 (1983).